Cement and Concrete Research 120 (2019) 256–266

Contents lists available at ScienceDirect

Cement and Concrete Research

journal homepage: www.elsevier.com/locate/cemconres

Physical evidence of swelling as the cause of anomalous capillary water uptake by cementitious materials

N.M. Alderete[a,b,*], Y.A. Villagrán Zaccardi[b], N. De Belie[a]

[a] Magnel Laboratory for Concrete Research, Department of Structural Engineering, Faculty of Engineering and Architecture, Ghent University, Tech Lane Ghent Science Park, Campus A, Technologiepark Zwijnaarde 60, B-9052 Ghent, Belgium
[b] LEMIT, CONICET, 52 entre 121 y 122 s/n, 1900 La Plata, Argentina

ARTICLE INFO

Keywords:
Swelling
Calcium silicate hydrate (C-S-H)
Sorptivity
Wetting strain

ABSTRACT

Water uptake by capillarity is widely used for characterising the durability properties of building materials. However, cementitious materials are generally reported with an anomalous behaviour in relation to other construction materials: during capillary water uptake they show a non-linear evolution with the square root of time. Several hypotheses have been proposed to explain this anomaly, among which the most sound seems to be the hygroscopic nature of cementitious materials, since the swelling of the calcium silicate hydrates when in contact with water could limit the water flow. Using strain gauges attached to mortar and concrete samples, we monitored their deformations during capillary water uptake. This paper presents those results and their connection with water ingress. Experimental data registered during water uptake allow validating the swelling hypothesis. The idea of cementitious materials as rigid materials during capillary water uptake seems incomplete for a comprehensive description of the transport process.

1. The anomalous capillary water uptake by cementitious materials

Water uptake by capillary forces is a transport property widely used for characterising the resistance to ingress of aggressive agents that are transported with water. Sorptivity, usually defined as the a measure of the capacity of the material to absorb a liquid by capillarity, is a good descriptor of several transport properties, since it is related to pore structure and connectivity. In the literature, there are several examples of relationships between sorptivity (generally expressed in units of mass/area/time$^{0.5}$) and other durability and transport properties such as drying rate (DR) [1], chloride diffusion [2], water penetration under pressure [2–4], resistance against freeze and thaw [5–7]. Consequently, sorptivity is primarily used as a qualitative descriptor of the durable performance of concrete when exposed to environmental aggressiveness.

Despite the good correlation between sorptivity and other transport properties, its calculation requires to implement certain conventions to obtain a sorptivity value. This is reflected in the different ways by which standards deal with its calculation [8–12]. The main reason for these differences is that the transport process does not evolve linearly with the square root of time, $t^{0.5}$, in cementitious materials, which is an anomaly not shared with other building materials. Several hypotheses have been built to explain it: electroviscous effects (changes in apparent viscosity during the filling process), modifications of contact angle factors [13], gravity effects [14], heterogeneous moisture content inside the sample [15], leaching of calcium hydroxide into the water [16], and swelling [13,17,18]. Gravity effects are established as the cause of anomalous behaviour in certain extremely coarse-pored cementitious materials, but this cannot be applied in general terms to all cementitious materials. A comprehensive evaluation of this issue leads to the consideration of the hygroscopic nature of cementitious materials (i.e. their affinity for moisture). The interaction of the calcium silicate hydrate (C-S-H) gel with water causes swelling and this may be the main cause inducing the deviation from the relationship with $t^{0.5}$. Villagrán et al. [18] presented an extensive analysis of this lack of linearity considering the hypotheses aforementioned and reached the conclusion that swelling seems to be the most sound explanation. Furthermore, the theoretical model presented in [18] describes the transport process by capillarity in cementitious materials progressing linearly with $t^{0.25}$. A main hypothesis for this model is the development of swelling at a sufficient rate so it can affect the water uptake rate. Capillary

* Corresponding author at: Magnel Laboratory for Concrete Research, Department of Structural Engineering, Faculty of Engineering and Architecture, Ghent University, Tech Lane Ghent Science Park, Campus A, Technologiepark Zwijnaarde 60, B-9052 Ghent, Belgium.
E-mail addresses: NataliaMariel.Alderete@UGent.be (N.M. Alderete), YuryVillagran@conicet.gov.ar (Y.A. Villagrán Zaccardi), Nele.DeBelie@UGent.be (N. De Belie).

https://doi.org/10.1016/j.cemconres.2019.04.001
Received 17 September 2018; Received in revised form 30 March 2019; Accepted 1 April 2019

absorption in swelling porous materials in general has been addressed by several authors, and in this sense two general approaches can be considered. As explained in [18,19], the hydraulic diffusivity (D) might be considered as a separable function of the moisture content (θ) and time (*t*), as in Eq. (1). Then, it is necessary to define γ to reflect the evolution of the hydraulic diffusivity. Considering that volumetric expansion varies linearly with $t^{0.5}$, it leads to the fourth root of time approach [18]. Then, measurements of deformation caused by swelling could provide new insights into the transport process. However this approach seems useful from a practical point of view, it should be considered merely empirical due to the fact that it uses the fractional diffusion equation formulated for rigid media for analysing absorption in swelling media [20]. Some inconsistencies for the value of D arising when γ is made equal to $0.5{\cdot}t^{-0.5}$, as suggested by experimental results, are therefore natural.

$$D(\theta, t) = \gamma(t) \bullet \delta(\theta) \tag{1}$$

where D is the hydraulic diffusivity, θ is the moisture content,γ is the time-varying diffusivity factor, δ is the saturation-varying diffusivity factor, and *t* is the time.

A more comprehensive alternative to the previous model is the application of the general sub-diffusion model, Eq. (2), as derived by Su [20] from the equations governing flow in swelling media formulated in a material coordinate, x, by Philip and Smiles [21–23] and the fractional derivative model by Zhang et al. [24]. In this case, the material diffusivity is defined in relation to moisture content only, and the inconsistencies derived from defining a variation with *t* are avoided.

$$\frac{\partial^{\beta}\vartheta}{\partial t^{\beta}} = \frac{\vartheta}{\vartheta_x}\left(D_x \frac{\partial \vartheta}{\partial_x}\right) 0 < \beta < 1 \tag{2}$$

where D_x (ϑ) is the hydraulic diffusivity in swelling media, ϑ is the moisture ratio equal to θ_l/θ_s, with θ_l and θ_s the volume fractions of liquid and solid, respectively, and *x* is the material coordinate.

Finally, the cumulative absorption by the swelling material is given as Eq. (3) [20], with S being the anomalous sorptivity of the material.

$$I(t) = S \bullet t^{\beta/2} \tag{3}$$

Imbibition is the displacement of one fluid by another with greater wettability than the first one [25]. This can be seen from food industry to construction, soils engineering, and etcetera. Alava et al. [26] provided a list with a wide range of scenarios in which imbibition plays a role. Spontaneous capillary imbibition takes place when the invading fluid does so under the only influence of capillary forces, with no external pressure [27]. According to the literature in physics, imbibition does not necessarily cause a change in volume, so imbibition in porous materials may or may not involve swelling. However, in the case of capillary water uptake in seeds, imbibition describes the particular action of taking up fluid resulting in swelling [28]. For the case of capillary imbibition in cementitious materials, the binding of water also implies swelling because of the hygroscopic nature of C-S-H. Additionally, unhydrated cement particles can react when in contact with water and further hinder the water flow. A mathematical model considering the hydration of unreacted cement particles has been proposed by Chapwanya et al. [30]. They consider that the anomalous behaviour of cementitious materials is mainly due to the reaction of the 'residual reactants', which clog the pores inside concrete thus hindering water transport. This model, although interesting, requires the input of several parameters to determine the reaction rate of the unhydrated cement particles and it does not consider swelling of the already formed C-S-H gel as a possible cause of the anomalous behaviour. Expansion due to water absorption has been measured by Hall et al. [13], and it was connected to the interaction between incoming water and C-S-H. Other authors have also suggested that changes in microstructure may occur when water enters the cementitious matrix [19,31–33], with a reduction in the flow rate as a consequence. In [34], based on single-sided ^{1}H nuclear magnetic resonance results, evidence of swelling is presented and clearly connected with a reduction in coarse porosity of pre-dried samples. Such modification of the microstructure does not occur when testing with organic liquids, in these cases no expansion and linear evolution of capillary uptake with $t^{0.5}$ was reported in [35].

A difference between the swelling of cementitious materials and of seeds is that the expansion of the latter is not as restricted as in the case of cementitious materials. Actually, the deformations depend on the amount of restrictions provided by the presence of non-deforming phases. During capillary imbibition, the swelling in cementitious materials is mainly translated into an increased tortuosity of the system (or 'pore disconnection'). Thomas and Jennings [36] showed that if the degree of restraint (with values 0 = no restraint and 1 = full restraint) is higher than a value numerically equivalent to the initial volume fraction of pores, porosity will reduce due to expansion. This results in a variation in pore structure geometry as the water front advances. Considering a partially restrained three-phase composite: deforming matrix phase, non-deforming inclusions, and pores; the deformation of the composite will be influenced by the degree of restraint in the composite and the relative volume fraction of the phases. If there are no restraints in the system, pores will deform in the same way as the total external dimensions of the composite. If the composite is fully restrained, the deformation (swelling) of the solid phase will cause pores to shrink. Based on relations between the initial pore volume and the degree of restraint [36], a system with a higher porosity will need a larger level of restraint to avoid pore volume increase. In the case of mortar and concrete, the amount of non-deforming phase will be given by the amount of aggregates in each case. Deformation determinations on mortar and concrete can provide information about the relation between pore volume and restraints.

From a physical point of view, there is no reason to believe that a single value for β originates from swelling during water absorption in any cementitious material. It is more likely that β varies from system to system within a certain range of values. However, a fair linear correlation with $t^{0.25}$ has been empirically confirmed by extensive experimental data analyzed in a previous work [18]. The error associated with considering a single value for the exponent seems therefore acceptable, considering the practical benefit of having S as the only parameter needed for describing capillary water absorption in cementitious materials. This approximation is extremely convenient for practitioners dealing with capillary water absorption of cementitious materials, whereas the defining factors for the particular value of the exponent can be further investigated.

In this investigation, an experimental set-up was designed to demonstrate the effect of the water ingress on the volumetric stability of mortar and concrete samples. The deformations registered during capillary imbibition are an external indication of swelling. These deformations also allow validating the swelling hypothesis to explain anomalous capillary imbibition in cementitious materials when the internal restrictions are considered.

2. Materials

To prepare the mortar mix, ordinary Portland cement (OPC) CEM I 42.5 N, tap water, and normalized sand with grain sizes ranging from 0 mm to 2 mm were used. The mortar mix was designed with a water to cement ratio of 0.45 and a sand to cement ratio of 3. The mixing procedure was performed in accordance with EN 196-1 [37]. Three prismatic samples of 160 mm × 40 mm × 40 mm were cast to evaluate the compressive strength of the mortar mix. Cylinders of 75 mm height and 50 mm in diameter were cast for the capillary imbibition test. Five samples were tested, as from an statistical analysis this amount was found to provide a good balance between precision and practicality [38]. To limit the effect of bleeding, cylindrical samples were kept rotating horizontally in sealed moulds during the first 24 h after casting. After 24 h, all samples were demoulded and placed inside a conditioned

Table 1
Concrete mix composition, air content, and slump.

Materials	Cement (kg/m^3)	Water (kg/m^3)	Sand (kg/m^3)	Gravel 2/8[a] (kg/m^3)	Gravel 8/16[b] (kg/m^3)	Air content (%)	Slump (cm)
Amount	339	152	813	524	623	2.5	11.5

[a] Nominal size between 2 and 8 mm.
[b] Nominal size between 8 and 16 mm.

room at (95 ± 5) % RH and (20 ± 1) °C until testing.

To prepare the concrete mix, the same cement and water to cement ratio were used. The concrete mix composition, air content, and slump are displayed in Table 1. To improve the workability, a commercially available polycarboxylic ether-based superplasticiser was added to the concrete during mixing. The product information indicated an optimal dosage between 4.5 ml and 13 ml per kg of cement. An intermediate dosage was chosen. The mixing procedure was made as follows: first cement, fine and coarse aggregates were dry-mixed for a minute; then the water was added and the mixing continued for 2 more minutes, finally the superplasticiser was added and mixed for 1 extra minute. The consistency was measured according to EN 12350-2 [39]. The air content was measured according to [39]. Values of the slump and air content are shown in Table 1. Five cylinders of 200 mm height and 100 mm in diameter were casted for the capillary imbibition test. Three cubic samples of 150 mm were also cast to evaluate the compressive strength. All samples were placed inside a conditioned room at (95 ± 5) % RH and (20 ± 1) °C until testing.

After curing for 28 days, all mortar and concrete samples were taken out of the conditioned room. The compressive strength of mortar samples was determined in accordance with EN 196–1 [37], resulting in an average value of 51 MPa. From the mortar cylinders, the bottom 25 mm were removed. These cylinders, with final height = 50 mm, were used for the capillary imbibition test (Fig. 1). The water absorption under vacuum and the open porosity of the mortar samples were 6.9% and 14% respectively.

The compressive strength test of concrete samples was performed in accordance with NBN B 15-220 [40], the mean compressive strength of the concrete samples at 28 days was 55 MPa. A slice between 30 mm and 80 mm from the bottom was cut off the cylinders. These 50 mm high samples were used for the capillary imbibition test (Fig. 1). The water absorption under vacuum and the open porosity of the concrete samples were 4.8% and 11.9% respectively.

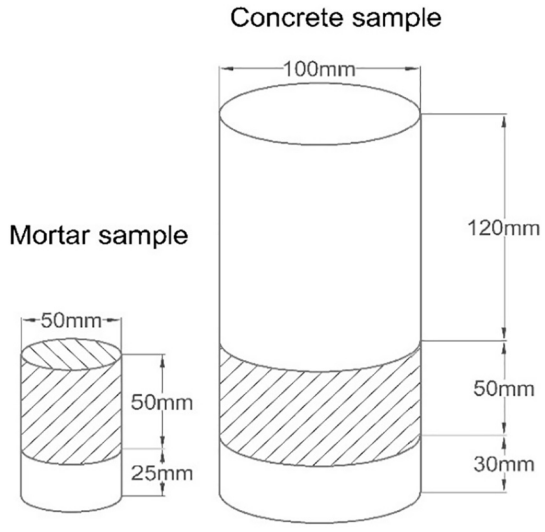

Fig. 1. Dimensions of mortar and concrete samples used for the capillary imbibition tests. The dashed volumes are the part of the samples used.

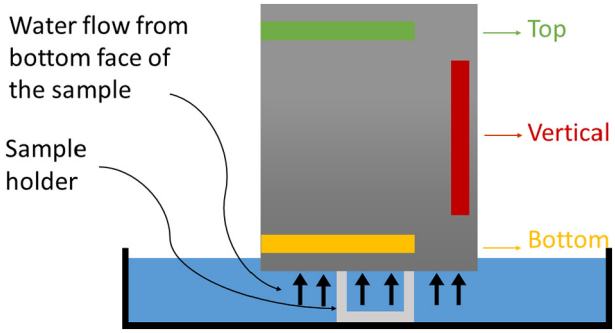

Fig. 2. Position of the strain gauges on the sample (not to scale).

3. Experimental set-up

To measure the deformation of the samples when exposed to water, general purpose strain gauges were used. These were strain gauges with linear pattern for use on concrete (from Micro Measurements -VPG). Two sizes of strain gauges were used: 60 mm × 4.78 mm (long strain gauge) and 20 mm × 4.78 mm (short strain gauge) in overall length and overall width, respectively. Three strain gauges were attached to each of the samples: a long one in horizontal position at 3 mm from the bottom (yellow), another long one in horizontal position at 3 mm from the top (green), and a short one vertically (red) (Fig. 2).

3.1. Mortar samples

Mortar samples were first pre-conditioned and then the strain gauges were attached to them. Samples were kept under immersion for 72 h and afterwards they were dried in an oven at 50 °C until their weight loss was lower than a mass fraction of 0.1% in a 24 h period. This preconditioning took approximately 8–9 days, with no less than three additional days with the samples sealed in plastic bags until the start of the test.

A specific purpose adhesive was applied to attach the strain gauges to the mortar surface and to ensure a proper strain transmission. Cables were connected to the strain gauges by soft soldering. The cables were then attached to a 3-pin wire connector and connected to other cables linked to the data logger. Continuous recording of the deformation was made automatically by an appropriate software. Fig. 3 shows the experimental set-up designed to monitor volumetric stability of mortars during capillary imbibition (left), and the strain gauges attached to a mortar sample (right).

After the adhesive reached its maximum strength (24 h), mortar samples were covered around their circumference with a double layer of paraffin tape to avoid evaporation and ensure one-dimensional flow of water. The semi-transparent paraffin tape was chosen to monitor any possible damage to the strain gauges during the capillary imbibition test. All five samples were connected to the automatic and continuous recording system previous to exposure to water to have a 'baseline' reading. This measurement was later used in the calculations to discount the noise inherent to the apparatus. After 5 min, samples were put in a container in contact with water, with an immersion depth of (3 ± 1) mm. The container was covered in order to avoid water evaporation.

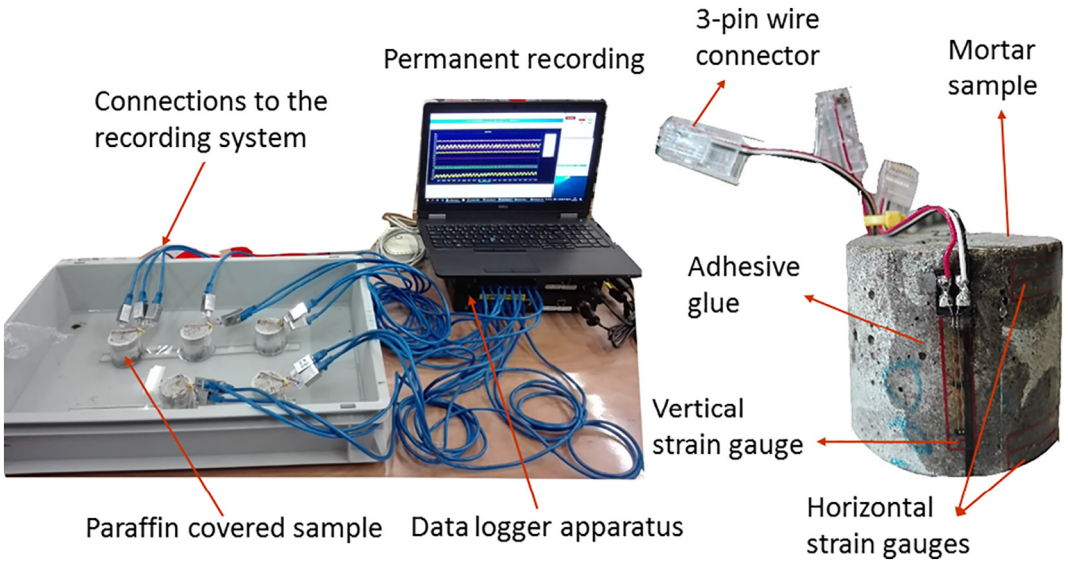

Fig. 3. Experimental set-up to monitor volumetric stability of mortars during capillary imbibition. Position of the strain gauges on a mortar sample (right), mortar samples during continuous measurement of deformations (left).

Along with the deformation recordings, gravimetric measurements were performed after 0.5 h, 1 h, 2 h, 3 h, 4 h, 5 h, 6 h, 24 h, and every 24 h during the first week. Then, gravimetric measurements were made every week for a total period of one month.

3.2. Concrete samples

Three strain gauges were adhered to each concrete sample in the same position as in the mortar samples (two horizontally placed and one vertically placed). The same kind of strain gauges and connections as described for mortars was used to measure the deformation of the concrete samples when exposed to water. Furthermore, a thermocouple was attached to one sample to monitor any temperature change and make the corresponding thermal expansion corrections of the strain gauges. Given that some strain gauges broke during the measurements in mortar samples, a specific purpose coating was applied on the strain gauges to protect them from contact with liquid water. After this coating, instead of using paraffin tape to cover the lateral surfaces of the samples, two layers of a thixotropic two-component epoxy resin (SikaCor-277®) were applied on the lateral surfaces of the samples (Fig. 4).

The preconditioning of the concrete samples was made after the strain gauges were attached. This was done to evaluate the volumetric changes during the whole process that involves the capillary imbibition tests. All five samples were connected to the automatic and continuous recording system previous to exposure to water to have a 'baseline' reading. This measurement was later used in the calculations to discount the noise inherent to the apparatus. After 5 min, samples were put under immersion for 72 h. Then, samples were taken out of immersion and placed in an oven at 50 °C until the mass decrease was lower than a mass fraction of 0.1% within 24 h. During drying, along with the deformation recordings, gravimetric measurements were performed after 0.5 h, 1 h, 2 h, 3 h, 4 h, 5 h, 6 h, 24 h, and every 24 h until constant mass was achieved (which took eight days). After the preconditioning period ended, samples were taken out of the oven, sealed in double plastic bags and kept in a conditioned room at (20 ± 1) °C for a week. This was done to achieve a uniform moisture distribution in the whole sample. Subsequently, samples were connected to the data logger for five minutes to obtain a new 'baseline' reading. These values were later used in the calculations to discount the noise inherent to the apparatus. Samples were put in contact with water, with an immersion depth of (3 ± 1) mm and the capillary imbibition test was performed for 12 weeks. The gravimetric measurements were performed after 0.5 h, 1 h, 2 h, 3 h, 4 h, 5 h, 6 h, 24 h, and every 24 h during the first week. Then, gravimetric measurements were made every week for a total period of three months.

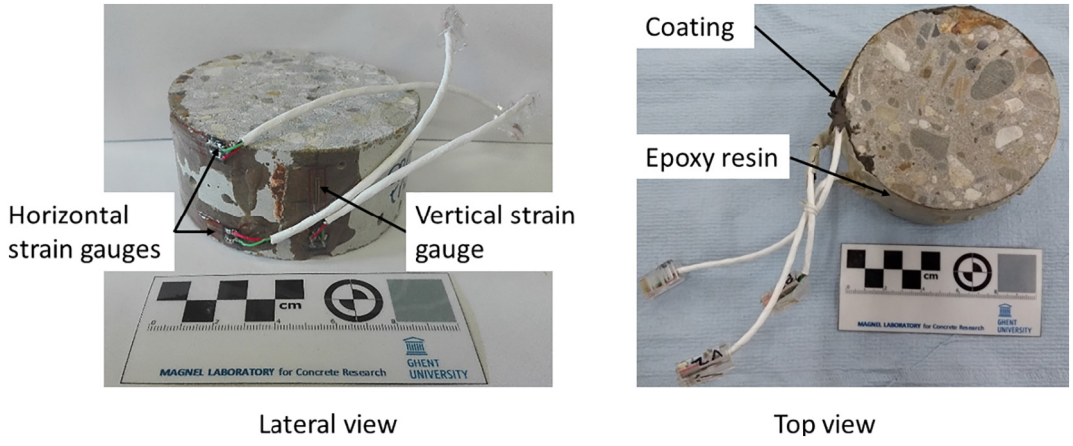

Fig. 4. Lateral and top view of a concrete sample before and after the application of the coatings, respectively.

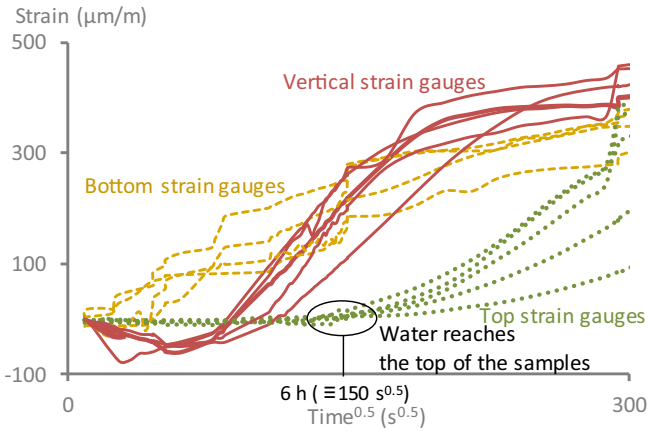

Fig. 5. Deformation measurements of mortar samples after 24 h of contact with water. Dashed yellow lines, full red lines, and dotted green lines correspond to the measurements from the bottom, vertical, and top strain gauges, respectively, of each of the samples. (For interpretation of the references to colour in this figure legend, the reader is referred to the web version of this article.)

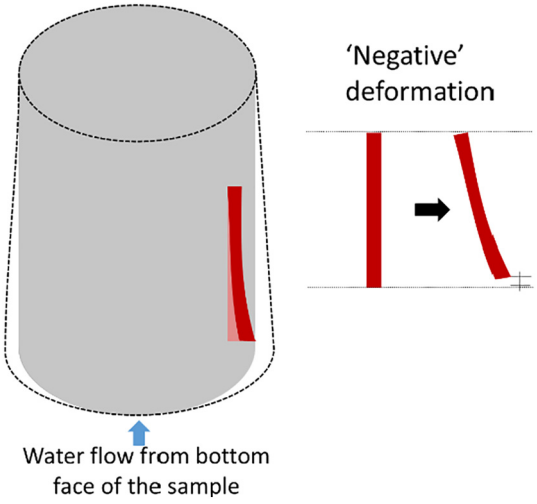

Fig. 6. Contraction experienced by a vertical strain gauge during the first hours of measurements (not to scale).

4. Results and discussion

4.1. Mortar

4.1.1. Deformations measured in mortar samples during the first 24 h of capillary imbibition

Fig. 5 shows the measurements registered over the first 24 h of contact with water in relation with the square root of time, in s$^{0.5}$. Strains are represented on the left vertical axis. Dashed yellow lines, full red lines, and dotted green lines in Fig. 5 correspond to the measurements from the bottom, vertical, and top strain gauges, respectively, of each of the samples. Fig. 5 shows four dashed yellow lines instead of five because one of the bottom strain gauges became defective when it got in contact with liquid water, due to insufficient protection of the cover glue. The bottom strain gauges were placed right above the water line (not immersed). However, it is possible that insufficient attachment of the paraffin on the bottom caused the variability seen at the beginning of the measurements. The scatter of data is significant but consistent with the type of measurements under study. With this in mind, the analysis of results is made from a conceptual and qualitative point of view, and no quantifications are possible at this point.

Strain gauges placed at the bottom started to register deformations (dashed yellow lines) right after contact with water. This indicates that the water ingress has almost an instant effect on the volume change of the samples. Because of the hygroscopic nature of C-S-H, water uptake produces immediate swelling of the bottom of the sample as it is exposed to water. From the first contact with water until approximately 24 h (≡293 s$^{0.5}$) all bottom strain gauges registered positive deformations (expansion).

Dotted green lines, corresponding with the top strain gauges, show no registry of deformation during the first 6 h (≡150 s$^{0.5}$). This is in fact a measurement of the water ingress rate, as the time at which the top strain gauges started registering deformations corresponds to the time needed for the moisture flow to go through the height of the sample. From 6 h to approximately 24 h, a continuous deformation increase was registered. The continuous increase in the deformations indicates a progressive increase in the water content at the top of the sample rather than a uniform advancing water front. Correspondingly, studies of neutron radiography made on mortar samples show the lack of a sharp water front during the first hours of capillary imbibition [41].

The measurements of the vertical strain gauges, full red lines, registered negative values in the beginning of the test, which represent a contraction in the generatrix of the sample (Fig. 6). This is related to the expansion produced only at the bottom of the sample at the start of the test. Therefore, the vertical strain gauge slightly reduces its length. Later, as water passes through the samples, this produces a progressive expansion along the height of the sample and then the vertical strain gauge starts to measure positive deformations.

The registered deformations during capillary imbibition are consistent with the evolution of the moisture content as water moves higher into the sample. Fig. 7 shows a schematic representation of the volumetric changes suffered by a mortar sample during the first hours of the capillary imbibition test, where three stages can be differentiated. The grey dashed lines represent the magnified deformed shape of the samples to visualize the deformations. Stage I induces the instantaneous expansions at the bottom of the sample and the contraction suffered by the rest of the matrix. During stage II, the rise of the water level

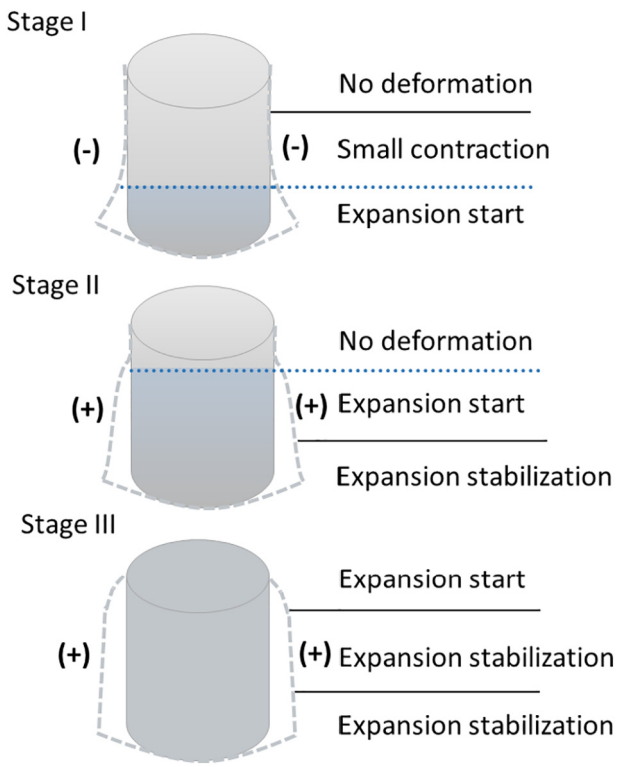

Fig. 7. Scheme of the volumetric changes suffered by the mortar sample during the first hours of the capillary imbibition test (not to scale).

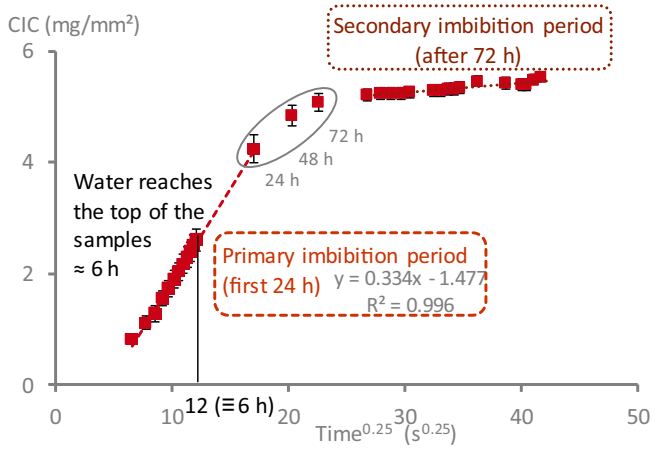

Fig. 8. Capillary imbibition capacity of mortar samples plotted against the fourth root of time.

increases deformation along the sample and balances the negative deformations registered in stage I. Stage III could be defined as the moment in which the water flow reaches the top of the samples. At this point the top strain gauges start to record the volumetric changes induced by the water ingress.

Deformation evolving with the square root of time is consistent with the anomalous capillary water uptake, on the supposition that hydraulic diffusivity evolves in direct correlation with these volumetric changes. The external indication can reflect a reduction of the hydraulic diffusivity when the balance between internal restriction and porosity is considered [36]. More experimental data is needed for an accurate quantification of the effect of swelling on the capillary water uptake rate, but the results presented here demonstrate that capillary water uptake should progress linearly with t^{α}, with $\alpha < 0.5$ when swelling occurs in combination with internal restriction (see Section 4.3).

4.1.2. Gravimetric measurements of mortar samples

Fig. 8 shows the variation of the capillary imbibition capacity (CIC) plotted as a function of the fourth root of the time. The equation of the fitting line as well as the coefficient of determination (R^2) are indicated in the figure for the primary imbibition period. The slopes of the fitting line represent the primary (CIR) imbibition rate. CIR has a very good correlation (> 0.99) with $t^{0.25}$, which indicates that the transport process occurs with variable hydraulic diffusivity (in contrast, the linear correlation with $t^{0.5}$ is 0.978). For the CIR, our hypothesis sustains that the pore network defines the CIR upon its affectation by swelling coupled with internal restriction. For the secondary imbibition rate (sCIR), the further increase in weight has been explained by a slow diffusion of air trapped during the primary period [42]. The exact value for β requires further studies, especially regarding a comprehensible statistical analysis. However, strong evidence on the suitability of the $t^{0.25}$ approach has been presented in [18,43], and having a unique value for cementitious materials seems convenient for practical purposes.

The ingress of water into the cementitious matrix can be therefore divided in two periods: an initial or primary period ruled by capillary forces, and a secondary period in which diffusion seems to be the governing phenomenon. As water enters into the samples, capillary forces drive its movement until the top of the samples is reached. That moment (about 6 h or 12 $s^{0.25}$) indicates the end of the dominant capillary imbibition phenomena, as almost no further water rise is possible. It seems that there is a transition between the water flow dominated by capillary forces and the following water ingress. During this transition, the capillary potential is increasingly reduced as the water front approaches the top face. Note that this division is different from the one stated in the standard ASTM C1585-13 [44], which refers to a relationship to $t^{0.5}$ instead of $t^{0.25}$. In Fig. 8, the points of this transition are marked with ellipses and correspond to 24 h, 48 h, and 72 h for the tested samples. The ellipses indicate the measurements that were collected during the period in which the top face of the samples started to be wet (this was detected by visual inspection). Then, the reduction in the water uptake rate reveals that the wet front has fully covered the height of samples.

During this 'transition' period (between 24 h and 72 h) there is a conversion between the main driving forces acting during the transport process. After 72 h, there is a significantly decreased slope caused by further imbibition without water rise. In this secondary period, there is a change in the dominating transport process as there is no longer a capillary potential (height of samples has been completely covered). The following increase in water content in the sample is generally explained by slow diffusion of air trapped during primary absorption [42], with a consequential redistribution of moisture from the capillary pores towards finer pores. This secondary process takes place at a lower rate than the CIR. This considerably slow process during the secondary imbibition period can be explained by strong joining forces present in consolidated C-S-H interlayer spaces and intraglobular pores as a result of previous drying [34].

4.1.3. Correlation between gravimetric measurements and deformations after 1 month of continuous recording

As discussed, the measurements of the deformations during the first 24 h of capillary imbibition show that water ingress does have an effect on the volumetric stability of the samples. The time at which the top strain gauges started registering deformations (≈6 h) provided information about the water ingress rate. Those results are in agreement with the gravimetric measurements. A comparison between the progress of the water ingress and the registered deformations during a month is presented in Fig. 9. The CIC (right vertical axis) is plotted here as a function of the square root of time to be able to compare simultaneously the change in CIC to the change in the deformation curves. Strains are plotted on the left vertical axis. Some strain gauges became defective during the long-term measurements and stopped recording: one vertical strain gauge at 1692 $s^{0.5}$, one top strain gauge at 1694 $s^{0.5}$, and three bottom strain gauges at 839 $s^{0.5}$, 1017 $s^{0.5}$, and 1501 $s^{0.5}$.

Interestingly, the progress of the CIC can be correlated to the progress of deformations sample by sample. This is indicated in Fig. 9 considering the samples that had the lowest and the highest CIC (blue

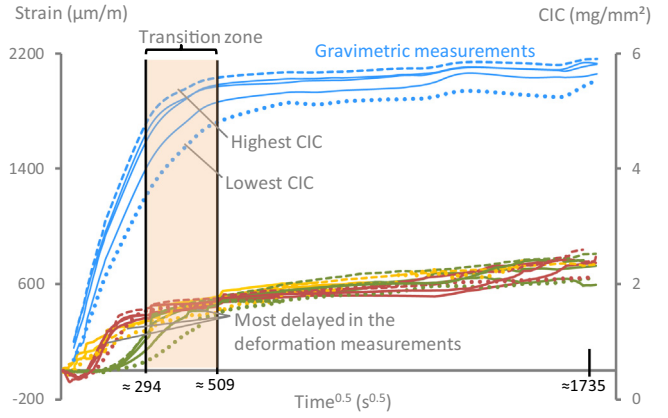

Fig. 9. Strain and CIC variation during the capillary imbibition test of mortar samples. Gravimetric measurements are represented on the right vertical axis (blue lines). Strain measurements are represented on the left vertical axis. Yellow, red, green, and blue lines correspond to the measurements from the bottom, vertical, and top strain gauges, and the gravimetric measurements, respectively. Dotted and dashed lines correspond to samples with the lowest and highest CIC, respectively. (For interpretation of the references to colour in this figure legend, the reader is referred to the web version of this article.)

dotted and blue dashed lines, respectively). The sample with the lowest CIC also had the most delayed recording of the deformations, as pointed out in the graph. The dotted green curve corresponds to the deformations on the top of that sample and, as it had a slow capillary rise, the water flow through that sample was the last to reach the top and make the face wet. This was the determining sample for the right limit of 'transition' period, marked in the graph at ≈509 $s^{0.5}$. Likewise, the dotted red and dotted yellow curves (vertical and bottom recordings, respectively) correspond to the sample with the lowest CIC. These curves also show a delayed registering of the deformations (marked in the graph), which is translated into a slower water ingress into the sample in comparison with the others. A similar analysis can be made for the sample with the highest CIC, marked with the dashed line in Fig. 9. The strain gauge from the top of this sample is the first to register deformations (green dashed line), which indicates that water flow has reached the top of this sample before the others. This is related to the highest CIR of this sample, when the dominating transport mechanism stops being capillarity. The green dashed line is also the one registering the highest deformation. The vertical strain gauge in this sample did not seem to be so much influenced by the corresponding CIC, although higher deformations are seen on the dashed red line before and during the 'transition' period.

4.2. Concrete

4.2.1. Results of deformation measurements during the preconditioning stage

Deformation measurements registered during the preconditioning stage reflect well the variation in the water ingress/egress into the sample. Fig. 10 shows the evolution of the strain for the different strain gauges (left vertical axis) and the gravimetric measurements (right vertical axis, blue square markers) with the square root of time. Dotted green lines and dashed yellow lines represent the top and bottom strain gauge recordings, respectively. Deformations from vertical strain gauges had a large variability and are not shown in the graph.

As soon as samples were immersed in water, top and bottom strain gauges started to record deformations (Fig. 10). This differs from the results obtained during capillary imbibition for mortar samples (Fig. 9), where only the bottom strain gauges recorded deformations during the first hours because then water could only ingress from the bottom of the samples. In this case, as samples were completely immersed, both top and bottom faces were exposed to water. Therefore, top and bottom measurements increase alike during the immersion stage.

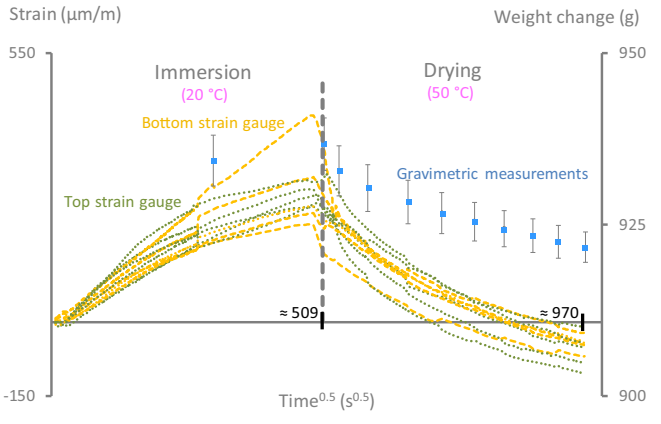

Fig. 10. Comparison between strain (left vertical axis, dotted green and dashed yellow lines for top and bottom strain gauges, respectively) and gravimetric measurements (right vertical axis, blue line) during preconditioning. Temperature measurements (dash-dot pink line) are represented on the left vertical axis. (For interpretation of the references to colour in this figure legend, the reader is referred to the web version of this article.)

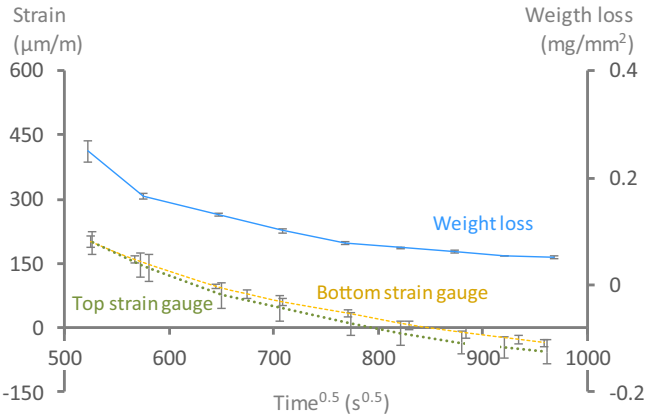

Fig. 11. Comparison between weight loss and strain measurements during drying at 50 °C in relation to $t^{0.5}$. Weight loss is represented on the right vertical axis (full blue line), and strain measurements are represented on the left vertical axis (dotted green and dashed yellow lines for top and bottom strain gauges, respectively). (For interpretation of the references to colour in this figure legend, the reader is referred to the web version of this article.)

After 72 h, samples were disconnected, removed from immersion, and taken to an oven at 50 °C (this took approximately 1 h). Then, they were connected back to the data logger and recordings started again. During drying, as water was removed from the sample, bottom and top strain gauges showed progressive contraction, since both bottom and top surface were exposed. Note that the comparison between weight change and deformations is made with $t^{0.5}$. This is because water loss does not hinder the transport as water ingress, as already mentioned in [18]. The external deformations during drying are well correlated with the gravimetric measurements, this can be seen in more detail in Fig. 11, where the average of weight loss and top and bottom deformations during drying at 50 °C are shown. Error bars represent the standard deviation (n = 5). Furthermore, it seems that the gravimetric measurements reach a relatively stable condition faster than the deformation measurements. However, it is likely that because of the high precision of the strain gauges, small deformations are still registered even after the mass loss is lower than 0.1% in a 24 h period. In relative terms, the later removal of interlayer water would cause more shrinkage than weight loss.

4.2.2. Gravimetric measurements of concrete samples

Results of the capillary imbibition test of concrete samples during three months are shown in Fig. 12. The equation of the fitting line as well as the coefficient of determination (R^2) are indicated in the figure

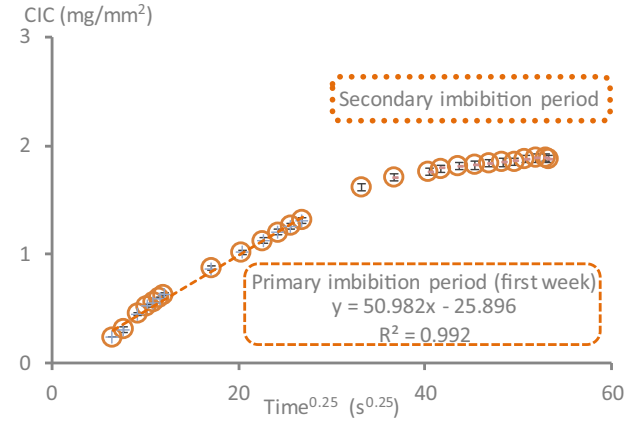

Fig. 12. Capillary imbibition capacity of concrete samples plotted against the fourth root of time.

for the primary period where a very good correlation, > 0.99, was found (in contrast, the linear correlation with $t^{0.5}$ is 0.95). The very early data (first two measurements) do not evolve perfectly linear with $t^{0.25}$. This irregularity can be explained by the setup of the absorption test, which requires a minimal submersion of approximately 3 mm for assuring good contact between the sample and the source of water. Only during the first minutes, the water ingress is therefore slightly accelerated by the minimal hydrostatic pressure. The effect is more visible in concrete than in mortar, as the sorptivity of the former is lower and the relative impact of the permeability on the mass increase is higher. The ingress of water into the concrete samples can also be divided in two periods: an initial or primary period that lasted approximately one week, and a secondary period starting to develop after three weeks. Each of these periods has a good relation with $t^{0.25}$ but with a different rate. The division between these periods is defined by the marked change in slope. This change is probably caused by the modification in the main driving force during the transport process. After the main water flow has reached the top of the sample, the forces driving transport and causing mass gain can no longer be capillary forces, as already discussed for the case of mortar samples.

4.2.3. Correlation between gravimetric and deformation measurements during 3 months of continuous recording

Fig. 13 shows the CIC and strain variation of concrete samples in function of $t^{0.5}$, during 3 months of continuous capillary imbibition monitoring. On the right vertical axis, gravimetric measurements are represented with full blue lines. On the left vertical axis, strain measurements are represented with dotted green, dashed yellow, and double dot - dash lines for top, bottom, and vertical strain gauges, respectively.

Similarly to results obtained from mortar samples, bottom strain gauges started registering deformations almost as soon as the samples were put in contact with water. Again, this is explained by the hygroscopic nature of the C-S-H, which interacts with the water flow and produces almost immediate volumetric variations. This is the cause of the deceleration seen in cementitious materials. Vertical strain gauges suffered a slightly negative deformation at the beginning of the test, but this was rapidly balanced with the positive deformations. Top strain gauges only started to record deformations after 24 h. This is in contrast with the measurements in the mortar samples, where top deformations were registered after 6 h. If concrete samples had had a greater height than mortar samples, the flow would have taken longer to reach the top of the sample. However, this is not the case, as both concrete and mortar samples had approximately 50 mm height. Discussion of possible causes for this difference is provided in the following section.

4.3. Comparison between deformations measured on mortar and concrete samples

Results of deformations during capillary imbibition show that mortar samples deform more than concrete samples. This discrepancy between mortar and concrete deformations may be attributed to several factors: (i) porosity and/or pore structure, (ii) C-S-H amount, and (iii) restriction of the system. Regarding (i), as the mortar phase composition of the concrete mix is similar to the one of mortar samples (same sand to cement ratio, same water to cement ratio, same cement, no supplementary cementitious materials), then differences in porosity can be mainly attributed to the presence of aggregates. One probable explanation is the fact that concrete mixes have a relatively lower paste volume than mortar mixes (i.e., the increased content of rather impermeable aggregates in concrete further restrict water flow). On the other hand, the interfacial transition zone between cement paste and aggregates offers a preferential pathway for transport [45]. The presence of aggregates would allow a more rapid water flow in that sense. Regarding (ii), the amount of C-S-H directly influences the deformations, as this is the main phase with a hygroscopic nature causing swelling and volumetric variations. In this regard, concrete samples have a lower relative amount of C-S-H than mortar samples. To take the influence of (i) and (ii) into account, the results of concrete samples were normalized to the volume of mortar contained in them. This was made by dividing the obtained deformation in concrete by the relative content of mortar in it (56%). By considering coarse aggregate as fully rigid, all the deformation that concrete suffers can be attributed to its mortar phase. Then, the normalized strain is the deformation that the mortar phase in concrete would develop when restrained by aggregates. It should be noted that the mortar in concrete cannot be considered completely the same as the mortar samples due to the effects of mixing, bleeding and the presence of additional interfacial transition zone. However, the comparison allows contrasting the degree of restraint in each material and contributes to the analysis of consistency of the results. Fig. 14 shows the average values and standard deviations of the deformations measured on mortar samples and the normalized deformations measured on concrete samples after one month. At least three strain gauges are considered for each series (some were broken during testing, as previously mentioned).

Deformations of the mortar phase contained in concrete samples are much lower than deformations in mortar samples. This is mostly a reflection of the level of constraint provided by the presence of rigid aggregates in concrete. As concrete has a higher level of internal constraint, the swelling of the C-S-H is more restricted than in mortar. With larger internal restriction, most of the deformation is translated in

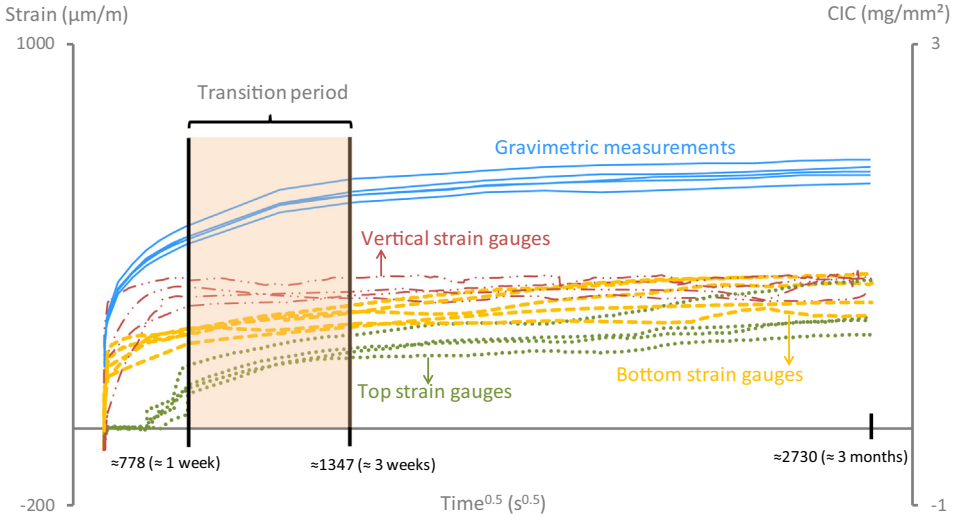

Fig. 13. Strain and CIC variation during the capillary imbibition test of concrete samples. Gravimetric measurements are represented on the right vertical axis (full blue line). Strain measurements are represented on the left vertical axis (dotted green, dashed yellow, and double dot -dash red lines for top, bottom, and vertical strain gauges, respectively). (For interpretation of the references to colour in this figure legend, the reader is referred to the web version of this article.)

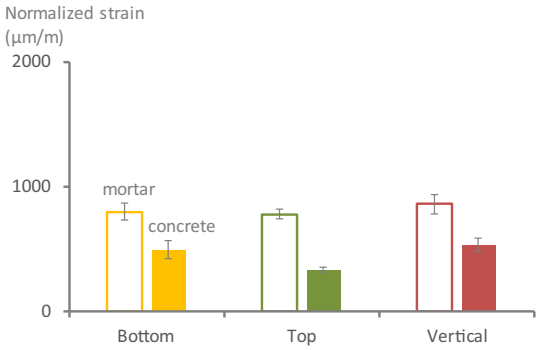

Fig. 14. Comparison between mortar deformations and (normalized) concrete deformations after one month of capillary imbibition. Empty/full columns represent deformations measured in mortar/concrete samples.

reducing the pore spaces rather than externally as in the case of free deformations. The impact of swelling on the imbibition rate is therefore directly linked to the content of non-deforming phases, such as aggregates (or inversely linked to the paste content). A similar case, but with opposite strains, is represented by the differences in shrinkage behaviour of paste, mortar and concrete. Toledo Filho et al. [46] found that cement paste has a higher drying shrinkage than concrete where the volume changes are largely restrained by the rigidity of the aggregates. Moreover, Thomas and Jennings [47] stated that the tendency of concrete to develop cracking due to shrinkage is an evidence of the large restrains that the embedded cement paste suffers.

In conclusion, the most influential parameter concerning the difference in deformations seems to be the restriction of the system in relation with its porosity. Considering a partially restrained three-phase composite: deforming matrix phase, non-deforming inclusions, and pores; Thomas and Jennings [36] proposed to describe the deformation of the composite by Eq. (2).

$$K_{tot} = K_{def} X_{def} + X_{nondef} + K_p X_p \quad (2)$$

where K_{tot} = ratio of final to initial volumes of the composite, K_{def} = ratio to final and initial volumes of the deforming phase, X_{def} = initial volume fraction of the deforming phase, X_{nondef} = initial volume fraction of the non-deforming phase, K_p = ratio to final and initial volumes of the porosity, X_p = initial volume fraction of pores.

The degree of restraint in the composite and the volume fraction of the phases will influence the relationship between K_p and K_{def}. If there were no restraints in the system, pores would deform in the same way as the total external dimensions of the composite. If the composite is fully restrained, the deformation of the solid phase would cause pores to shrink. There is a certain threshold degree of restraint that results in no change in pore size, $K_p = 1$, leading to Eq. (3):

$$K_{tot} = 1 + X_{def}(K_{def} - 1) \quad (3)$$

The expression provided in Eq. (3) characterises a limit in which the overall deformation of the composite and the deformation of the deforming phase are such that the pore size does not change [36]. This can be written as the following inequalities:

$$K_{tot} \begin{cases} < 1 + X_{def}(K_{def} - 1), & \text{pores shrink} \\ > 1 + X_{def}(K_{def} - 1), & \text{pores grow} \end{cases}$$

The variation of the pore volume ratio, K_p, varies with the deforming phase volume ratio, K_{def}, for a given amount of restraint. Moreover, the relation between K_{tot} and K_{def} provides the degree of restraint in a system. If there is complete restraint, there is no volume variation and $K_{tot} = 1$. If there are no restraints in the system, pores deform in the same way as the total external dimensions of the composite and $K_p = K_{tot}$. However, under restrained conditions, it is possible to consider a parameter R_d, called degree of restraint [36]. For a system without restraint $R_d = 0$, and for a fully restrained system $R_d = 1$. Then, the relation between K_{tot} and K_{def} can be expressed by Eq. (4).

$$K_{tot} = 1 + (1 - R_d)\left\{\left[\frac{K_{def} X_{def} + X_{nondef}}{(1 - X_p)}\right] - 1\right\} \quad (4)$$

Most interestingly, there is a threshold value of R_d (R_t) for which there are no changes in the pore volume ($K_p = 1$). This value can be expressed by combining Eqs. (3) and (4), which results in $R_t = X_p$. This indicates that R_t is numerically equivalent to the initial pore volume. A system with a higher porosity will need a larger level of restrain to avoid pore volume increase.

For considering the influence of swelling on the pore structure, it is important to verify if the total porosity shrinks as a result of swelling in the system contrary to the normal situation whereby pores would expand with its host matrix. Based on the aforementioned model proposed by [36], the degree of restraint was calculated for the case of the mortar samples considering that the deforming solid phase is the C-S-H (including the inherent gel pores). The rest of the solid phases of the paste and the fine aggregates were considered as non-deforming phases. From the volume that would represent the paste phase of the mortar (17%), the volume of the hydration products and the gel porosity was calculated with the model of Powers [48] (65%). The hydration degree was assumed to be $\alpha = 0.75$, based on results of field emission scanning electron microscopy performed on cement pastes with 28 days of curing provided in [49]. The volume fractions obtained of the deforming phase, non-deforming phase and porosity are $X_{def} = 0.154$, $X_{nondef} = 0.696$, and $X_p = 0.15$, respectively. Considering the deformations measured, the value of K_{tot} (ratio of final to initial volumes of the material) was found to be equal to 1.002, the value of K_{def} (ratio of the final to initial volumes of the deforming phase) for which the pore size does not change was found to be = 1.016. Given that the C-S-H swelling is certainly higher than 1.6% [34,50], (as a reference value it can be considered that Taylor estimates an expansion of 34% for C-S-H when going from dry state equilibrated at 11% RH to the saturated state [51]), this means that the pores shrink. In the case of concrete, the presence of coarse aggregates would offer both lower porosity and larger restrictions, and therefore the computations are even more conclusive in showing that the degree of restraint in the cementitious matrix is such that pores shrink when the deforming phase expands. It is important to mention that pore reduction should not be associated with a higher potential capillary rise as a consequence of smaller pore diameter. The effect of pore 'refinement' due to the restrictions of the system is mainly translated into an increased tortuosity. Hence, the water flow will be hindered as it encounters some restrictive pore sizes. As cement paste is not a homogeneous material, pores will not reduce uniformly either.

The measurements of deformation during the capillary imbibition tests, confirmed that volumetric changes are largely affected by the affinity of C-S-H with water. During the immersion stage, again the effect of the hygroscopic nature of C-S-H resulted in swelling immediately when in contact with water. During drying, deformations had a direct relation with the water loss. This is in agreement with the central concept of the model (CM-II) proposed by Jennings [52], where C-S-H are globules with water in three locations: adsorbed on the outer surface as a monolayer, adsorbed within the particle, and located in the interlayer space, capable of causing swelling and offering certain internal strains. This swelling will hinder the water flow only if a certain restriction degree is achieved. In fact, the final effect on the pore structure can be linked to three parameters described before: (i) porosity, (ii) amount of C-S-H, and (iii) restrictions in the system (actually (i) and (iii) are related, as discussed). In relation to (ii), if there is no C-S-H (or any hygroscopic component), the water flow will follow a linear variation with the square root of time, as it is the case for bricks or plaster. However, when C-S-H is present, its deformation makes the

pore structure to change as water advances, hence the anomalous behaviour of cementitious materials. This is also the case for cementitious materials with superabsorbent polymers, Snoeck et al. [53] found that during capillary imbibition tests, as SAP particles attract water, the permeation is lowered in those pores due to swelling of SAP.

4.4. The variation in deformations during the primary and secondary imbibition periods

The results of capillary imbibition in mortar and concrete samples confirm the difference in the water uptake between the primary and secondary imbibition periods. Water flow takes longer to reach the top of the concrete than the mortar samples and hence the diffusion process starts to increase its influence before the maximum capillary rise is reached. As the CIR and sCIR in concrete are lower than in mortar, they are also more comparable to the transport rate by diffusion. This is expected due to the lower porosity that concrete mixes have and also due to the higher constraints that the presence of coarse aggregates entails. Then, the transition between the primary and secondary imbibition periods is more gradual in concrete than in mortar. As water enters in the concrete sample, the deforming phase of the matrix is highly restrained, then it deforms towards the pores leading to an increased tortuosity and reduced hydraulic diffusivity.

Most deformations were registered during the primary period, both in mortar and concrete samples. This reflects in a way the activity of the C-S-H gel, as after the transition period, deformation measurements are much more stable than during the primary imbibition period. Regarding the secondary imbibition period, even though sCIR can be obtained from the linear relationship between mass increase and $t^{0.25}$, swelling does not have a major impact on this rate. Considering the analogy with the bilinear flow, the first stage is dominated by water being absorbed in macropores, whereas the second part is associated with transport along a linear pathway (gel pores). After the maximum capillary rise is achieved, the increase in weight would be associated to diffusion of water molecules into the laminar structure of C-S-H.

5. Conclusions

During exposure, the anomalous sorptivity of cementitious materials is connected with the water retention in the C-S-H structure (and consequent swelling) during the water flow. The delaying process linked with swelling is fast enough to show significant influence on the water flow rate due to capillary imbibition. In this sense, it is important to note that such an effect is possible from a combination of swelling and internal restriction in the material. An important message is that the consideration of cementitious materials as rigid materials seems incomplete for a comprehensive description of the transport process. The CIR is therefore better defined as the ratio between the water uptake and the fourth root of time, in comparison with the correlation with $t^{0.5}$ usually established, and this has been mainly attributed to the hygroscopicity of cementitious materials and swelling caused by the interaction with water coupled with internal restriction offered by non-deforming phases, mainly aggregates. The definition of the CIR as the rate of water uptake progressing over t^{α}, with $\alpha < 0.5$ potentially solves the usual problem of lack of linearity observed with the square root of time. In this regard, this paper presented additional results with a good fit with the $t^{0.25}$ approach; and, more importantly, from the measurement of strain during the process, it provided effective physical support to the swelling theory by which the anomalous capillary imbibition can be explained.

The experimental set-up designed to measure the deformations during the capillary imbibition test demonstrated the effect of the water ingress on the volumetric stability of mortar and concrete samples. All strain gauges were able to measure deformations as water progressed during capillary imbibition. The largest amount of deformations occurs during the primary imbibition period, indicating that swelling can explain the reduction in hydraulic diffusivity during capillary imbibition. A consistent correlation between deceleration of the CIR and external expansion is obtained when internal restriction and swelling are considered.

Mortar and concrete mixes were compared considering the normalized deformations, and the difference in the values could be related (at least partially) to the additional restraint that the mortar phase underwent in concrete samples. Even considering the normalized deformations, the mortar phase of concrete deforms less than mortar samples. The presence of coarse aggregate particles as non-deforming inclusions results in lower deformations because of the larger restraint. From estimations made contrasting pore volume and restraint, it was found that swelling causes pore size reduction. Therefore, the relative impact of swelling is greater in concrete than in mortar, as the smaller external deformation observed in concrete reflects a more significant pore 'refinement' than in mortar. These changes in the pore structure hinder the water flow, as its main effect is an increase in the tortuosity of the system.

Long-term capillary imbibition tests in concrete mixes manifested the existence of primary and secondary periods. The contrast between concrete and mortar regarding the impact of swelling can also explain the gradual transition from the primary to the secondary period. A deeper look into the secondary imbibition period is still needed.

Acknowledgements

The constructive criticism of anonymous reviewers is greatly appreciated by the authors as it has contributed greatly to the improvement of this paper.

References

[1] Y.A. Villagrán Zaccardi, N.M. Alderete, A. Píttori, Á.A. Di Maio, Drying rate as a transport index for concrete, XIII Conf. Durab. Build. Mater. Components, 2014, pp. 336–343.
[2] Y.A. Villagrán Zaccardi, V.L. Taus, A.A. Di Maio, Apreciaciones sobre el uso de parámetros prescriptivos para asegurar la durabilidad de estructuras de hormigón armado en ambiente marino, in: C.L.C. Andrade, E. Menéndez, L. Lima (Eds.), 1er. Simp. Técnico Iberoam. Sobre Estructuras y Mater. Para La Construcción, RILEM, Consolider SEDUREC, UNNOBA, AAHES, Buenos Aires, Argentina, 2010, pp. 36–53.
[3] P.A.M. Basheer, D.P. Rankin, G.I.B. Russell, Design of concrete to resist carbonation, in: M.A. Lacasse, D.J. Vanier (Eds.), 8th Int. Conf. Durab. Build. Mater. Components, 1999, pp. 423–435.
[4] P. Van den Heede, E. Gruyaert, N. De Belie, Transport properties of high-volume fly ash concrete: capillary water sorption, water sorption under vacuum and gas permeability, Cem. Concr. Compos. 32 (2010) 749–756, https://doi.org/10.1016/j.cemconcomp.2010.08.006.
[5] G.C. Long, K.L. Ma, Y.J. Xie, Water sorptivity and permability of new-old concrete composite system, Adv. Mater. Res. 163–167 (2011) 3311–3319, https://doi.org/10.4028/www.scientific.net/AMR.163-167.3311.
[6] C. Hazaree, K. Wang, H. Ceylan, K. Gopalakrishnan, Capillary transport in RCC: water-to-cement ratio, strength, and freeze-thaw resistance, J. Mater. Civ. Eng. 23 (2011) 1181–1191, https://doi.org/10.1061/(ASCE)MT.1943-5533.0000284.
[7] D.P. Bentz, M. a Ehlen, C.F. Ferraris, E.J. Garboczi, Sorptivity-based service life predictions for concrete pavements, 7th Int. Conf. Concr. Pavements–Orlando, Florida, USA, Sept. 1, 2001, pp. 9–13.
[8] ASTM C 1585, Standard Test Method for Measurement of Rate of Absorption of Water by Hydraulic-Cement Concretes, (2004).
[9] EN 13057, Products and Systems for the Protection and Repair of Concrete Structures - Test Methods - Determination of Resistance of Capillary Absorption, (2002).
[10] EN ISO 15148, Hygrothermal Performance of Building Materials and Products - Determination of Water Absorption Coefficient by Partial Immersion, (2003).
[11] EN 12808-5, Grouts for Tiles - Part 5: Determination of Water Absorption, (2009).
[12] EN 480-5, Admixtures for Concrete,Mortar and Grout - Test Methods - Part 5: Determination of Capillary Absorption, (2005).
[13] C. Hall, W.D. Hoff, S.C. Taylor, M.A. Wilson, B.-G. Yoon, H.-W. Reinhardt, et al., Water anomaly in capillary liquid absorption by cement-based materials, J. Mater. Sience Lett. 14 (1995) 1178–1181.
[14] C. Hall, T.K.M. Tse, Water movement in porous building materials-VII. The sorptivity of mortars, Build. Environ. 21 (1986) 113–118, https://doi.org/10.1016/0360-1323(86)90017-X.
[15] L.J. Parrott, Water absorption in cover concrete, Mater. Struct. 25 (1992) 284–292.
[16] H. Jennings, J. Kropp, K. Scrivener, Modelling of Microstructure and its Potential for Studying Transport Properties and Durability, 1st editio, Kluwer Academic Publishers, Boston, 1996.

[17] N.S. Martys, C.F. Ferraris, Capillary transport in mortars and concrete, Cem. Concr. Res. 27 (1997) 747–760, https://doi.org/10.1016/S0008-8846(97)00052-5.
[18] Y.A. Villagrán Zaccardi, N.M. Alderete, N. De Belie, Improved model for capillary absorption in cementitious materials: progress over the fourth root of time, Cem. Concr. Res. 100 (2017) 153–165, https://doi.org/10.1016/j.cemconres.2017.07.003.
[19] D.A. Lockington, J.-Y. Parlange, Anomalous water absorption in porous materials, J. Phys. D. Appl. Phys. 36 (2003) 760–767.
[20] N. Su, Equations of anomalous absorption onto swelling porous media, Mater. Lett. 63 (2009) 2483–2485, https://doi.org/10.1016/j.matlet.2009.08.039.
[21] D.E. Smiles, M.J. Rosenthal, The movement of water in swelling materials, Aust. J. Soil Res. 6 (1968) 237–248.
[22] D.E. Smiles, Infiltration into a swelling material, Soil Sci. 117 (1974) 140–147.
[23] J.R. Philip, Hydrostatics and hydrodynamics in swelling soils, Water Resour. Res. 5 (1969) 1070–1077.
[24] Y. Zhang, D.A. Benson, D.M. Reeves, Time and space nonlocalities underlying fractional-derivative models: distinction and literature review of field applications, Adv. Water Resour. 32 (2009) 561–581, https://doi.org/10.1016/j.advwatres.2009.01.008.
[25] R. Masoodi, K.M. Pillai, Wicking in Porous Materials Traditional and Modern Modeling Approaches, CRC Press - Taylosr and Francis Group, Boca Raton, 2012, https://doi.org/10.1201/b12972-5 10.1201/b12972-5.
[26] M. Alava, M. Dubé, M. Rost, Imbibition in disordered media, Adv. Phys. 53 (2004) 83–175, https://doi.org/10.1080/00018730410001687363.
[27] K.S. Schmid, S. Geiger, Universal scaling of spontaneous imbibition for water-wet systems, Water Resour. Res. 48 (2012) 1–13, https://doi.org/10.1029/2011WR011566.
[28] J.D. Bewley, K.J. Bradford, H.W.M. Hilhorst, H. Nonogaki, Seeds: Physiology of Development, Dermination and Dormancy, 3rd editio, (2013) New York.
[30] M. Chapwanya, J.M. Stockie, W. Liu, A model for reactive porous transport during re-wetting of hardened concrete, J. Eng. Math. 65 (2009) 53–73, https://doi.org/10.1007/s10665-009-9268-0.
[31] M. Küntz, P. Lavallée, Experimental evidence and theoretical analysis of anomalous diffusion during water infiltration in porous building materials, J. Phys. D. Appl. Phys. 34 (2001) 2547–2554.
[32] P. Rucker-Gramm, R.E. Beddoe, Effect of moisture content of concrete on water uptake, Cem. Concr. Res. 40 (2010) 102–108, https://doi.org/10.1016/j.cemconres.2009.09.001.
[33] N. Fischer, R. Haerdtl, P.J. McDonald, Observation of the redistribution of nanoscale water filled porosity in cement based materials during wetting, Cem. Concr. Res. 68 (2015) 148–155, https://doi.org/10.1016/j.cemconres.2014.10.013.
[34] R. Schulte Holthausen, M. Raupach, Monitoring the internal swelling in cementitious mortars with single-sided1H nuclear magnetic resonance, Cem. Concr. Res. 111 (2018) 138–146, https://doi.org/10.1016/j.cemconres.2018.05.021.
[35] M. Sosoro, Transport of organic fluids through concrete, Mater. Struct. 31 (1998) 162–169, https://doi.org/10.1007/BF02480390.
[36] J.J. Thomas, H.M. Jennings, Changes in the size of pores during shrinkage (or expansion) of cement paste and concrete, Cem. Concr. Res. 33 (2003) 1897–1900, https://doi.org/10.1016/S0008-8846(03)00167-4.
[37] NBN EN 196-1, Methods of Testing Cement - Part 1: Determination of Strength, Bur. Voor Norm, 2016.
[38] N. Alderete, Y.A. Villagrán-Zaccardi, A.A. Di Maio, Determinación de la velocidad de succión capilar del hormigón a partir de diferentes números de especímenes, VI Congr. Int. La AATH, 2014, pp. 295–302.
[39] EN 12350-7, Testing Fresh Concrete. Air Content. Pressure Methods., Bur. Voor Norm, (2009), p. 18.
[40] NBN B 15-220, Concrete Testing - Compressive Strength, Bur. Voor Norm, 1990, p. 6.
[41] N.M. Alderete, Y.A. Villagrán Zaccardi, D. Snoeck, B. Van Belleghem, P. Van Den Heede, K. Van Tittelboom, et al., Capillary imbibition in mortars with natural pozzolan, limestone powder and slag evaluated through neutron radiography, electrical conductivity, and gravimetric analysis, Cem. Concr. Compos. submitted (2018).
[42] M. Mainguy, O. Coussy, V. Baroghel-Bouny, Role of air pressure in drying of weakly permeable materials, J. Eng. Mech. 127 (2001) 582–592.
[43] Y. Villagrán-Zaccardi, N. Alderete, Á. Di Maio, LA GANANCIA DE PESO POR ABSORCIÓN CAPILAR, VIII Congr. Int. - 22a Reun. Técnica La AATH, AATH, Olavarría (Arg.), 2018, pp. 335–344.
[44] ASTM C1585-13, Standard Test Method for Measurement of Rate of Absorption of Water by Hydraulic Cement Concretes, vol. 41, ASTM Int., 2013, pp. 1–6, https://doi.org/10.1520/C1585-13.2.
[45] J. Lizarazo-Marriaga, C. Higuera, P. Claisse, Measuring the effect of the ITZ on the transport related properties of mortar using electrochemical impedance, Constr. Build. Mater. 52 (2014) 9–16, https://doi.org/10.1016/j.conbuildmat.2013.10.077.
[46] R.D. Toledo Filho, K. Ghavami, M.A. Sanjuán, G.L. England, Free, restrained and drying shrinkage of cement mortar composites reinforced with vegetable fibres, Cem. Concr. Compos. 27 (2005) 537–546, https://doi.org/10.1016/j.cemconcomp.2004.09.005.
[47] J.J. Thomas, H.M. Jennings, A colloidal interpretation of chemical aging of the C-S-H gel and its effects on the properties of cement paste, Cem. Concr. Res. 36 (2006) 30–38, https://doi.org/10.1016/j.cemconres.2004.10.022.
[48] H.J.H. Brouwers, The work of powers and Brownyard revisited: part 1, Cem. Concr. Res. 34 (2004) 1697–1716, https://doi.org/10.1016/j.cemconres.2004.05.031.
[49] H.S. Wong, N.R. Buenfeld, Determining the water-cement ratio, cement content, water content and degree of hydration of hardened cement paste: method development and validation on paste samples, Cem. Concr. Res. 39 (2009) 957–965, https://doi.org/10.1016/j.cemconres.2009.06.013.
[50] A.M. Gajewicz, E. Gartner, K. Kang, P.J. McDonald, V. Yermakou, A 1H NMR relaxometry investigation of gel-pore drying shrinkage in cement pastes, Cem. Concr. Res. 86 (2016) 12–19, https://doi.org/10.1016/j.cemconres.2016.04.013.
[51] H.F.W. Taylor, Cement Chemistry, 2nd ed., Thomas Telford Publishing, London, 1997.
[52] H.M. Jennings, Refinements to colloid model of C-S-H in cement: CM-II, Cem. Concr. Res. 38 (2008) 275–289, https://doi.org/10.1016/j.cemconres.2007.10.006.
[53] D. Snoeck, S. Steuperaert, K. Van Tittelboom, P. Dubruel, N. De Belie, Visualization of water penetration in cementitious materials with superabsorbent polymers by means of neutron radiography, Cem. Concr. Res. 42 (2012) 1113–1121, https://doi.org/10.1016/j.cemconres.2012.05.005.